Colligative Properties of Helical Polyelectrolytes

Jeffrey Skolnick*

Department of Chemistry, Yale University, New Haven, Connecticut 06520.
Received May 26, 1978

ABSTRACT: In the context of a continuum model, the excess electrostatic free energy, F_{excess}, of helical charge distributions has been obtained. More specifically, we calculate F_{excess} of α, DNA-like, and infinite pitch helical lines of charge embedded on the surface of a low dielectric cylinder. The deviation of F_{excess} from the uniformly charged cylinder value is evaluated as a function of screening length. The deviation is small for DNA, smaller for the α helix, and significant for the helix of infinite pitch. Moreover, employing the ideas of Manning, the colligative properties of such polyelectrolyte solutions have been obtained. The deviation from a line of charge in bulk solvent model is small at low salt concentration but becomes appreciable at higher ionic strengths.

In a recent paper,[1] hereafter designated paper 1, the Debye–Hückel equation was solved for the electrostatic interaction energy of point charges on the surface of a dielectric cylinder immersed in salt water; major deviations from the interaction in bulk solvent were found. We then applied the analytical results to calculate that portion of the potential, $\Delta\Psi$, of helical charge distributions which depends on salt concentration. For α and DNA-like helical charge distributions, the dominant contribution to $\Delta\Psi$ is the potential characteristic of a uniformly charged cylinder. In toto, the treatment of paper 1 indicated the large and at times surprising effect a low dielectric, salt-excluding cylinder can have on the electrostatic potential.

The present work deals with the calculation of $\Delta\Psi$ and various colligative properties of α, DNA-like, and infinite pitch helical charge distributions. Our approach is in the spirit of Manning,[2–4] and by analogy to simple electrolyte theory, the derived quantities have been designated extending Manning colligative properties. The reader is referred to paper 1 for a brief review of the literature.[1]

As a first approximation, it seems reasonable to view the helical polyion as a thin helical line of charge embedded on the surface of a low-dielectric, mobile, ion-free cylinder. α helices are represented by a single helical line of charge; DNA-type double helices are modeled by two helical lines of charge 180° out of phase with each other. When the pitch of the helix is infinite, the helix becomes a line of charge embedded on the surface of a low dielectric cylinder. Such a model is perhaps appropriate for linear, nonhelical polyelectrolytes[3] and is therefore examined.

A quantity of primary interest is the difference in reversible work required to charge up a given charge distribution in the presence and absence of salt, F_{excess}. The difference between the electrostatic free energy of a uniform charge distribution and the helical line is found to be rather small for either the α helix or for DNA but increases with increasing pitch and increasing salt concentration. Possibly, the difference might be significant for DNA at high salt concentrations. Although the dielectric cylinder exerts a drastic influence on the interaction between point charges, the effect has a different sign depending on whether the charges reside on the same or opposite sides of the cylinder, and there appears to be a significant cancellation for a helical charge distribution. However, over a considerable range of ionic strengths, major deviations in F_{excess} of the infinite pitch helix from both a line and uniform charge model are observed. As one would expect, the deviations become greater with increasing salt concentration.

* Address correspondence to this author at Bell Laboratories, Murray Hill, New Jersey 07974.

Since the deviations from ideality of polyelectrolyte colligative properties can be related to $(\partial F_{excess}/\partial\kappa)_{T,V}$, we determine this quantity for the α helix, line of charge, and DNA double helix. In each case, we delineate the conditions under which the line of charge in bulk solvent is the appropriate limiting case and when corrections become necessary. Finally, we formulate extended Manning colligative properties for the osmotic and activity coefficients of α helical, DNA-like helical, and infinite pitch helical polyelectrolytes.

The Excess Electrostatic Free Energy and Colligative Properties of Helical Charge Distributions

A. Description of the Model. In view of the quite large effect of a cylinder on the interaction between point charges on its surface,[1] especially at high salt concentration, we have examined the self-energy of helical distributions of charges. Specifically, one of the questions put in this section is whether the effect of varying salt concentration on the self energy differs between the helical array and a uniform charge distribution. The self energy is independent of the internal dielectric constant for the uniform distribution.

Having isolated that portion of the self energy which depends on salt concentration, F_{excess}, we then consider the influence of the helical charge distribution on the colligative properties of the polyelectrolyte solution. For α and DNA-like helical lines, our numerical work indicates that the difference in electrostatic free energy between the helical and uniform distributions is rather small. As Manning's limiting laws are easy to apply and represent a well-defined reference state,[2–4] it seems worthwhile to examine the predictions of Manning theory at finite salt concentration. Otherwise stated, we postulate the following at finite salt concentration: (I) If $\xi > 1$ counterions condense on the polyion to reduce ξ to one. Here, $\xi = q^2/D_2k_BTb$, where q is the protonic charge, k_B is Boltzmann's constant, T is the absolute temperature, b is the linear distance between charges in the configuration of maximum extension, and D_2 is the bulk solution dielectric constant. A 1:1 supporting electrolyte is assumed to be present. (This is Manning's assumption D.)[2] (II) We may treat the uncondensed ions in the Debye–Hückel approximation. (This is Manning's assumption E.)[2] (III) We neglect interactions between different polyions in the calculation of colligative properties. (IV) The helical polyelectrolyte is assumed to be infinitely long. (V) The helical polyelectrolyte is a salt-excluding, low-dielectric cylinder immersed in bulk solvent; the helical lines of charge reside on the surface.

Plausible rationalizations for assumptions I and II are as follows: First and foremost, we wish to define a simple

0024-9297/79/2212-0515$01.00/0

reference system valid at finite salt concentration. Furthermore, in some recent work, Manning[4] quotes a wealth of experimental data that supports the plausibility of assumption (I). For example, H. Skielman, J. M. A. M. van der Hoeven, and J. C. Leyte[5] performed some NMR studies on the sodium salts of polyphosphate, polyacrylate, and poly(styrenesulfonate) which indicate the existence of charge fractions, ξ^{-1}, at simple salt concentrations over 0.1 M. In the same paper, Manning[4] employed a discrete linear array of charges to calculate the electrostatic portion of the total free energy of the polyelectrolyte system. At finite salt concentration, C_S, such a model may not be appropriate for α and DNA helices, hence a partial motivation of the present approach. Moreover, Bailey[6] has summed the Mayer cycle diagrams and has concluded that assumptions I and II are accurate for $0.01 \leq C_S \leq 0.1$.

Recently, Stigter[7] has published a comparison of numerical solutions of the nonlinear Poisson–Boltzmann equation with Manning's counterion condensation theory. His work supports to some extent the results of MacGillivray and Winklemann[8] and MacGillivray[9,10] on the zero salt limit validity of Manning's theory. However, at finite salt and especially for $\xi > 1$, significant differences in the surface potential from predictions of counterion condensation theory are apparent. Clearly, work remains to be done to reconcile the differences between the Poisson–Boltzmann equation and counterion condensation approaches.

As charge screening increases with an increase in supporting electrolyte concentration, the neglect of polyion–polyion interactions, assumption III, should become a better approximation at finite salt concentration.

In the case of α helical and DNA-like helical polyelectrolytes, the infinite length approximation improves with increasing C_S. If the range of the electrostatic interaction is small relative to the length of a rodlike region, the neglect of end effects is valid. As both α helices and DNA have very large intrinsic persistence lengths, assumption IV is quite reasonable. When considering linear polyions (e.g., carboxymethylcellulose) that are approximated as infinite pitch helices, care should be taken to insure the above criterion is met.[11]

We conclude this section with a brief examination of assumption V. A primary purpose of this work is the investigation of the effect of a dielectric discontinuity on helical polyelectrolyte colligative properties. Hence, we have arbitrarily chosen the cylinder dielectric constant D_1 as 2; the bulk solvent dielectric constant, D_2, was taken to be 80. Moreover, we have placed the line of charge on the surface of the dielectric cylinder. Based on the work of Bailey,[12] we observe that the actual location of the charge (in or on the cylinder) is unimportant in the determination of F_{excess} for α and DNA-like helical distributions. However, in the case of the infinite pitch helix,[13] whether the charge resides on or is embedded in the cylinder is significant. As the line of charge is placed closer to the center of the low dielectric region, those terms which represent the angular asymmetry in the potential become unimportant.[14] Consequently, the proposed infinite pitch helical model may be appropriate for those polyelectrolytes with large backbone radii, e.g., carboxymethylcellulose, but is perhaps unrealistic for small cylinder radii molecules such as poly(acrylic acid).

B. Calculation of F_{excess} and Some Colligative Properties. Let the jth charge in a helical array be located at z_j in the cylindrical polar coordinates $(z_j,a,\theta') = \mathbf{r}'$. Here, $\theta' = 2\pi z_j/p$ and the pitch of the helix is p. For an α helix, p/a is about 0.68 and for a DNA-like helix, P/a is about 3.45. When the pitch is infinite, the helix becomes a line of charges parallel to the cylinder axis.

In paper 1 we solved the linearized Poisson–Boltzmann equation for the potential of a point charge on the surface of a mobile ion-free, low-dielectric cylinder. Whereupon, the potential Ψ_T arising from the interaction of two charges on the surface of the cylinder and a distance z apart[15] (with respect to the principal axis) is given from paper 1 (eq 2.11) by

$$\Psi_T = \frac{2q}{z\pi}\{H_0 + 2\sum_{n=1}^{\infty} H_n \cos n(\theta - \theta')\} \tag{1a}$$

$$H_n = z\int_0^{\infty} \mathrm{d}l h_n \cos (lz) \tag{1b}$$

$$h_n = \frac{-K_n(\lambda a)I_n(la)}{D_2\lambda a K_n'(\lambda a)I_n(la) - D_1 la K_n(\lambda a)I_n'(la)} \tag{1c}$$

The I_n and K_n are modified Bessel functions of the first and second kind.[1] The prime denotes the derivative with respect to the argument. Furthermore, a is the radius of the dielectric cylinder and $\lambda^2 = l^2 + \kappa^2$, where κ^{-1} is the Debye screening length:

$$\kappa^2 = \frac{4\pi q^2}{D_2 k_B T}\sum_i n_i v_i^2$$

$n_i \equiv$ number of ions of species i per cm^3 and v_i is the valence of the ith ion.

The potential Ψ at a given charge in the helical array is defined as the sum of the pairwise interactions Ψ_T

$$\Psi = \sum_j \Psi_T(\kappa,z_j) \tag{2}$$

The sums could be handled straightforwardly with the aid of methods presented in paper 1. It would be substantially easier if the sums could be converted to integrals; we shall modify eq 2 to permit this simplification. Before considering the continuum limit of eq 2, we note that corrections arising from the discrete nature of the charge distribution are expected when κb is on the order of unity. For a DNA helix, the discreteness of the distribution becomes important when $\kappa a \simeq 5.88$ or $C_S = 3.20$. C_S is the molar concentration of simple salt. These observations are confirmed by Bailey;[12] Bailey considered a discrete charge representation of DNA and found for C_S up to 1.1 M ($\kappa a = 3.3$ and $\kappa b = 0.6$) only small, salt-independent corrections to the uniformly charged cylinder surface potential. As we are interested in that part of Ψ which depends on salt concentration, the continuum limit of eq 2 should be a valid representation of the physics for $\kappa a \leq 2$.

As written, conversion to an integral would give the potential acting on a charge in a continuous helix, and this potential is infinite. We, therefore, add and subtract a comparison potential for vanishing salt concentration and write

$$\Psi = \Delta\Psi + \Psi^0 \tag{3}$$

$$\Psi^0 = \sum_j \Psi_T^0(0,z_j) \tag{4}$$

$$\Delta\Psi = \sum_j [\Psi_T(\kappa,z_j) - \Psi_T^0(0,z_j)] \tag{5}$$

If Ψ^0 were defined as the potential Ψ evaluated at $\kappa = 0$, the summand in eq 5 would be finite at $z = 0$ but would diverge for large z_j, whereupon the desired integral over z could not be extended to infinity. Consequently, Ψ^0 is defined as the potential for $\kappa = 0$ minus the potential of a uniformly charged cylinder at $\kappa = 0$. The subtraction is identical to an omission of the $n = 0$ term in eq 1a (the $n = 0$ term is proportional to $-\ln a$). We thus arrive at a

Table I[a]
$4\pi\Delta h_{n/n}$

κa	$4\pi h_0$	$n =$ 1	2	3	4	5	6
0.1	3.87E-01	-8.48E-07	-1.11E-07	-3.34E-08	-1.42E-08	-7.30E-09	-4.24E-09
0.2	2.88E-01	-3.39E-06	-4.44E-07	-1.34E-07	-5.68E-08	-2.92E-08	-1.70E-08
0.3	2.35E-01	-7.62E-06	-9.98E-07	-3.00E-07	-1.28E-07	-6.57E-08	-3.82E-08
0.4	2.00E-01	-1.35E-05	-1.77E-06	-5.34E-07	-2.27E-07	-1.17E-07	-6.79E-08
0.5	1.75E-01	-2.12E-05	-2.77E-06	-8.34E-07	-3.55E-07	-1.83E-07	-1.06E-07
0.6	1.56E-01	-3.04E-05	-3.99E-06	-1.20E-06	-5.11E-07	-2.63E-07	-1.53E-07
0.7	1.41E-01	-4.14E-05	-5.43E-06	-1.64E-06	-6.96E-07	-3.58E-07	-2.08E-07
0.8	1.29E-01	-5.40E-05	-7.09E-06	-2.14E-06	-9.08E-07	-4.67E-07	-2.71E-07
0.9	1.19E-01	-6.82E-05	-8.97E-06	-2.70E-06	-1.15E-06	-5.92E-07	-3.43E-07
1.0	1.10E-01	-8.41E-05	-1.11E-05	-3.34E-06	-1.42E-06	-7.30E-07	-4.24E-07
1.1	1.02E-01	-1.02E-04	-1.34E-05	-4.04E-06	-1.72E-06	-8.83E-07	-5.13E-07
1.2	9.59E-02	-1.21E-04	-1.59E-05	-4.80E-06	-2.04E-06	-1.05E-06	-6.10E-07
1.3	9.03E-02	-1.41E-04	-1.87E-05	-5.63E-06	-2.40E-06	-1.23E-06	-7.16E-07
1.4	8.52E-02	-1.64E-04	-2.17E-05	-6.53E-06	-2.78E-06	-1.43E-06	-8.31E-07
1.5	8.07E-02	-1.87E-04	-2.48E-05	-7.50E-06	-3.19E-06	-1.64E-06	-9.54E-07
1.6	7.67E-02	-2.13E-04	-2.82E-05	-8.53E-06	-3.63E-06	-1.87E-06	-1.09E-06
1.7	7.30E-02	-2.39E-04	-3.19E-05	-9.62E-06	-4.10E-06	-2.11E-06	-1.23E-06
1.8	6.98E-02	-2.68E-04	-3.57E-05	-1.08E-05	-4.59E-06	-2.36E-06	-1.37E-06
1.9	6.67E-02	-2.98E-04	-3.97E-05	-1.20E-05	-5.12E-06	-2.63E-06	-1.53E-06
2.0	6.40E-02	-3.28E-04	-4.40E-05	-1.33E-05	-5.67E-06	-2.92E-06	-1.70E-06

[a] $4\pi\Delta h_n$ as a function of n and κa for an α helix, $p/a = 0.68$, $D_1 = 2$, $D_2 = 80$.

definition of $\Delta\Psi$ which permits replacement of the sum by an infinite integral. As the reference potential, Ψ^0, is independent of salt concentration, $\Delta\Psi$ separates naturally into the potential of a uniform charge distribution and corrections that depend on the pitch.

Employing eq 1a in eq 4 and in the continuous limit, we find

$$\Delta\psi = \frac{\beta}{\pi}\sum_{n=-\infty}^{+\infty}\int_{-\infty}^{\infty} \mathrm{d}l \int_{-\infty}^{\infty} \mathrm{d}z (h_n - h_n^0) \exp[i(lz + n\phi)] \tag{6a}$$

Here β is the charge per unit length of axis, and

$$\phi = \theta + 2\pi z/p \tag{6b}$$

We have included a phase shift θ to incorporate the effect of the double stripe of charges in DNA. If $\theta = 0$, the $z = 0$ term should be omitted; if $\theta = 180°$, all charges are included in the sum.

Recognizing a delta function in eq 6a,

$$\delta(y) = (2\pi)^{-1}\int_{-\infty}^{\infty} \mathrm{d}z \exp[zy]$$

we have

$$\Delta\Psi = 2\beta\{h_0 + 2\sum_{n=1}^{\infty}\Delta h_n \cos n\theta\} \tag{7a}$$

$$\Delta h_n = h_n(2\pi n/p) - h_n^0(2\pi n/p), \quad n \geq 1 \tag{7b}$$

$$h_0 = K_0(\kappa a)/D_2\kappa a K_1(\kappa a) \tag{7c}$$

Here, the displayed argument of h_n is the value of l. A superscript zero implies $\kappa = 0$, and its absence indicates that the actual value of κ should be used.

In the calculation of colligative properties, the quantity of interest is the difference in reversible work done in charging up a helical distribution of charge in the presence and absence of salt, F_{excess}, and is related to $\Delta\Psi$ by[2]

$$F_{\text{excess}} = \int_0^L \mathrm{d}z \int_0^\beta \mathrm{d}\beta' \Delta\Psi(\beta') \tag{8}$$

Substitution of eq 7a into eq 8 and integration over z gives

$$F_{\text{excess}} = \frac{\beta^2 L}{D_2}\left\{\frac{K_0(\kappa a)}{\kappa a K_1(\kappa a)} + 2D_2\sum_{n=1}^{\infty}\Delta h_n \cos n\theta\right\} \tag{9}$$

The first term on the right-hand side of eq 9 is the excess electrostatic free energy of a uniformly charged cylinder of radius a. The second class of terms contains corrections to the excess free energy due to differences in the helical charge distribution from a uniform one. When the pitch p goes to zero, all $\Delta h_n = 0$ and we recover the uniformly charged cylinder result.

The colligative properties of the polyelectrolyte solution can be related to $(\partial F_{\text{excess}}/\partial\kappa)_{T,V}$[2]

$$\left(\frac{\partial F_{\text{excess}}}{\partial \kappa}\right)_{T,V} = \frac{\beta^2 L}{D_2\kappa}\left\{-1 + \frac{K_0^2(\kappa a)}{K_1^2(\kappa a)} + 2D_2\left(\frac{\partial(\sum_{n=1}^{\infty}\Delta h_n \cos n\theta)}{\partial \ln \kappa}\right)_{T,V}\right\} \tag{10}$$

The first term, proportional to -1, arises from the interaction of a line of charge immersed in bulk solvent with the mobile ions. The second term, proportional to $K_0^2(\kappa a)/K_1^2(\kappa a)$, contains corrections to $(\partial F_{\text{excess}}/\partial\kappa)_{T,V}$, resulting from the fact the helix is wrapped around a salt-excluding cylinder. For a fixed value of κ, it is an *increasing* function of κa. Increasing κa gives rise to a larger excluded salt effect and a concommitant increase in F_{excess}. The third class of terms are the corrections to F_{excess} due to the difference in the helical distribution from a uniform one. Included in ${}_pF_{\text{excess}}$

$${}_pF_{\text{excess}} = 2\beta^2 L \sum_{n=1}^{\infty}\Delta h_n \cos n\theta$$

are the effects of mobile ion screening. Hence, ${}_pF_{\text{excess}}$ should be a *decreasing* function of κa.

In the α helical case, $a = 7.5$ Å, $p = 5.1$ Å, and $\theta = 0°$. The required values of h_n are easily computed from eq 1c. Consultation of Table I readily verifies that to an excellent approximation

$$F_{\text{excess}}^{\alpha} = \frac{\beta^2 L}{D_2}\left\{\frac{K_0(\kappa a)}{\kappa a K_1(\kappa a)}\right\} \tag{11a}$$

and

$$\left(\frac{\partial F_{\text{excess}}^{\alpha}}{\partial \kappa}\right)_{T,V} = \frac{\beta^2 L}{D_2\kappa}\left\{-1 + \frac{K_0^2(\kappa a)}{K_1^2(\kappa a)}\right\} \tag{11b}$$

Table II[a]
$\beta^{-2}L^{-1}F^{\text{line}}_{\text{excess}}$ vs. κa

κa	uniform cylinder	$\theta = 0°$
0.1	0.3869	0.3792
0.2	0.2882	0.2657
0.3	0.2352	0.1951
0.4	0.2004	0.1418
0.5	0.1753	0.0981
0.6	0.1562	0.0608
0.7	0.1411	0.0281
0.8	0.1288	−0.0012
0.9	0.1186	−0.0278
1.0	0.1099	−0.0521
1.1	0.1024	−0.0745
1.2	0.0959	−0.0953
1.3	0.0902	−0.1148
1.4	0.0852	−0.1330
1.5	0.0807	−0.1502
1.6	0.0767	−0.1664
1.7	0.0730	−0.1818
1.8	0.0697	−0.1965
1.9	0.0667	−0.2105
2.0	0.0640	−0.2238

[a] For a helix of infinite pitch, D_2, the solvent dielectric constant was taken to be 80. D_1, the cylinder dielectric constant, was assumed to be 2.

Thus, for a continuous α helical distribution of charge, the excess electrostatic free energy is well approximated by that of a uniformly charged cylinder. Moreover, it is only in the limit that $\kappa a \to 0$ that the helical distribution appears as a line of charge.

In Figure 1, we plot $-C^{\alpha}(\kappa a)$ as a function of κa, where

$$-C^{\alpha}(\kappa a) = \frac{D_2}{\beta^2 L}\left(\frac{\partial F_{\text{excess}}{}^{\alpha}}{\partial \ln \kappa}\right)_{T,V} \tag{12}$$

If $\kappa a \geq 0.15$ or $C_S \geq 3.7 \times 10^{-3}$ M, we predict experimentally observable (greater than 5%) deviations in the colligative properties of α helices from a line of charge in the bulk solvent model.

If pitch is set equal to infinity, the helix reduces to a line of charge embedded on the surface of a low-dielectric, salt-excluding cylinder. This model may be relevant to linear, nonhelical polyelectrolytes such as carboxymethylcellulose.

Taking the limit of Δh_n in eq 7b as the argument of h_n goes to zero, i.e., the pitch, p, becomes infinite, it follows that[12]

$$F^{\text{line}}_{\text{excess}} = \frac{\beta^2 L}{D_2}\left\{\frac{K_0(\kappa a)}{\kappa a K_1(\kappa a)} + 2D_2 \sum_{n=1}^{\infty} \Delta h_n{}^{\text{line}}\right\} \tag{13a}$$

where

$$\Delta h_n{}^{\text{line}} = \left\{\left[n(D_1 + D_2) + \frac{D_2 \kappa a K_{n-1}(\kappa a)}{K_n(\kappa a)}\right]^{-1} - [n(D_1 + D_2)]^{-1}\right\} \tag{13b}$$

As previously, the first term on the right-hand side of eq 13a is the free energy associated with the reversible work done in charging up a uniformly charged cylinder. The second class of terms appears due to the angular asymmetry in the lines of flux induced by the presence of the low-dielectric, mobile, ion-free cylinder.

In Table II, we present $\beta^{-2}L^{-1}F^{\text{line}}_{\text{excess}}$ as a function of κa; discussion of the results is deferred until after $(\partial F^{\text{line}}_{\text{excess}}/\partial \kappa)_{T,V}$ has been calculated.

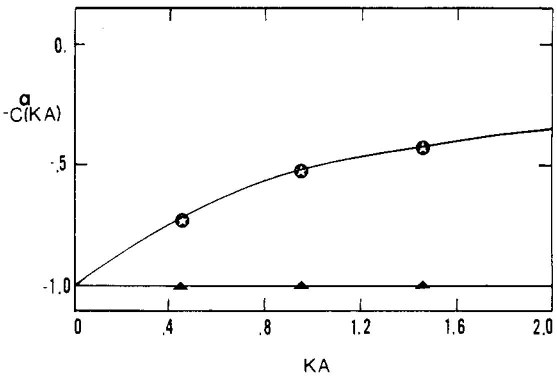

Figure 1. The triangles give the value of $-C^{\alpha}(\kappa a)$ as a function of κa, if the α helix were a line of charge in bulk solvent. The stars give the value of $-C^{\alpha}(\kappa a)$ from eq 12 and incorporate the salt excluding backbone effect into the colligative properties. p = 5.1 Å and a = 7.5 Å.

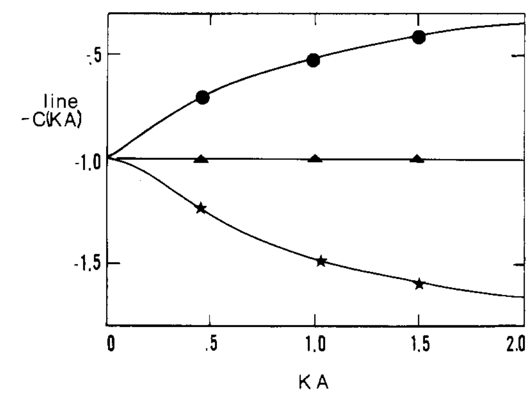

Figure 2. The stars give $-C^{\text{line}}(\kappa a)$, defined in eq 15, as a function of κa for a line of charge embedded on the surface of a low dielectric, $D_1 = 2$, cylinder; −1, the triangles, is the value if the line of charge were immersed in bulk solvent. The circles denote the uniformly charged cylinder contribution to $-C^{\text{line}}(\kappa a)$.

Table III[a]
a vs. $C_S{}^{\max}$

a, Å	$C_S{}^{\max}$, mol/L
1.25	0.133
1.75	0.069
3.0	0.023
13	0.0012

[a] a vs. the maximum salt concentration line of charge in bulk solvent adequately (within 5%) predicts the colligative properties of a helix of infinite pitch.

Taking the derivative of $F^{\text{line}}_{\text{excess}}$ with respect to κ we have

$$\left(\frac{\partial F^{\text{line}}_{\text{excess}}}{\partial \kappa}\right)_{T,V} = \frac{-\beta^2 L C^{\text{line}}(\kappa a)}{D_2 \kappa} \tag{14}$$

where

$$-C^{\text{line}}(\kappa a) = -1 + \frac{K_0{}^2(\kappa a)}{K_1{}^2(\kappa a)} + 2D_2\left(\frac{\partial(\sum_{n=1}^{\infty} \Delta h_n{}^{\text{line}})}{\partial \ln \kappa}\right)_{T,V} \tag{15}$$

In Figure 2 we plot $-C^{\text{line}}(\kappa a)$ as a function of κa. As expected, when $\kappa a << 1$, the dominant contribution to $(\partial F^{\text{line}}_{\text{excess}}/\partial \kappa)_{T,V}$ arises from the line of charge in the bulk solvent model. Provided that the cylinder's radius is very

Table IV[a]

κa	uniform cylinder	$\theta = 0$	$\theta = \pi$	av of $\theta + \pi$, i.e., $\Delta\Psi^{DNA}$
0.1	0.38690	0.38674	0.38701	0.38688
0.2	0.28823	0.28759	0.28869	0.28814
0.3	0.23515	0.23372	0.23618	0.23495
0.4	0.20037	0.19785	0.20217	0.20001
0.5	0.17532	0.17144	0.17810	0.17477
0.6	0.15624	0.15073	0.16016	0.15544
0.7	0.14112	0.13375	0.14634	0.14005
0.8	0.12881	0.11936	0.13546	0.12741
0.9	0.11856	0.10685	0.12674	0.11679
1.0	0.10987	0.09574	0.11968	0.10771
1.1	0.10242	0.08573	0.11391	0.09982
1.2	0.09594	0.07658	0.10916	0.09287
1.3	0.09025	0.06812	0.10523	0.08668
1.4	0.08521	0.06025	0.10197	0.08111
1.5	0.08072	0.05286	0.09925	0.07605
1.6	0.07668	0.04589	0.09697	0.07143
1.7	0.07304	0.03928	0.09507	0.06717
1.8	0.06973	0.03299	0.09346	0.06323
1.9	0.06672	0.02699	0.09212	0.05955
2.0	0.06396	0.02124	0.09098	0.05611

[a] For a DNA-like helix $p/a = 3.45$, $D_1 = 2$, $D_2 = 80$.

small relative to κ, the mobile ions essentially interact with a line of charge with a slight perturbation caused by the dielectric cylinder. However, when $\kappa a \geq 0.15$, there should be measurable deviations in $-C^{\text{line}}(\kappa a)$ from a line of charge in bulk solvent model. In Table III, we present the maximum salt concentration vs. cylinder radius for which the line of charge model in bulk solvent adequately characterizes the colligative properties of an infinite pitch helix.

Note that $-C^{\text{line}}(\kappa a)$ is a decreasing function of κa for a fixed value of κ. This may perhaps be rationalized by a qualitative arguement analogous to that for the two point charges (see the discussion at the close of section II in paper 1). First of all, it is those terms which reflect the angular asymmetry in the potential,

$$2D_2\left(\frac{\partial(\sum_{n=1}^{\infty}\Delta h_n^{\text{line}})}{\partial \ln \kappa}\right)_{T,V}$$

that dominate the difference in $(\partial F_{\text{excess}}^{\text{line}}/\partial\kappa)_{T,V}$ from -1. (The line of charge in bulk solvent results.) As previously, we argue that the lines of flux will tend to avoid the cylinder, the avoidance increasing with increasing κa. Whereupon, over a region of space opposite the line of charge ($\theta = 180°$), there is a decreased flux density from both the spreading of the lines of flux and their termination on counterions. Conversely, in that portion of space near ($\theta = 0°$) the line of charge, there is an increase in flux density vis-à-vis the absence of the dielectric cylinder. With respect to the line of charge in bulk solvent, the net effect appears to be a decrease in the excess reversible work required to charge up a helix of infinite pitch. Thus, the excess reversible work decreases with increasing angular asymmetry, i.e., increasing κa.

One further note is necessary: the qualitative conclusions of the infinite pitch helix result should hold for all $D_1 << D_2$; this calculation points out the qualitative importance of the low dielectric effect on the colligative properties.

We continue this section with an examination of the colligative properties of a DNA-type double helix. The charge distribution is modeled as two helical lines of charge, 180° out of phase with respect to each other. The lines of charge lie on the surface of a low-dielectric,

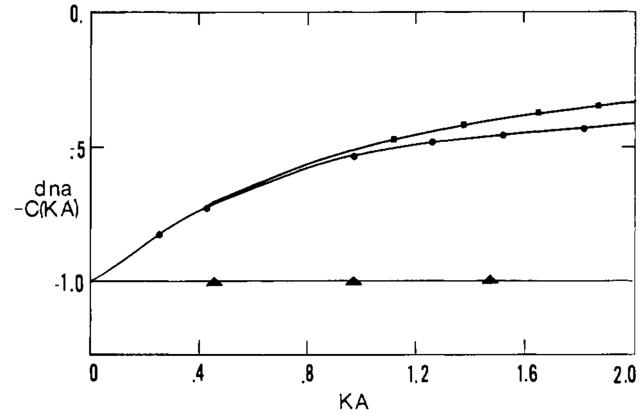

Figure 3. The circles give $-C^{\text{DNA}}(\kappa a)$, defined by eq 18b, as a function of κa. The squares represent the uniformly charged cylinder contribution to $-C^{\text{DNA}}(\kappa a)$; -1, the triangles, is the value for a line of charge in bulk solvent. $p/a = 3.45$.

salt-excluding cylinder. Thus, by eq 7a and by adding the potential of the two helical lines

$$\Delta\Psi^{\text{DNA}} = 2\beta\{h_0 + 2\sum_{n=1}^{\infty}\Delta h_n^{\text{DNA}}(1 + \cos(n\pi))\} \tag{16a}$$

β is the charge density per unit length of axis; in DNA the unit length of the axis is 1.7 Å. Clearly, only the even n contribute to the sum in eq 16a. Hence,

$$\Delta\Psi^{\text{DNA}} = 2\beta\{h_0 + 4\sum_{n=1}^{\infty}\Delta h_{2n}^{\text{DNA}}\} \tag{16b}$$

We have computed the Δh_{2n} from eq 7b. The corrections to the uniform charge distribution are extremely small for $\kappa a < 1.0$ as a brief consultation of Table IV will verify. Inserting eq 16b into eq 8 gives

$$F_{\text{excess}}^{\text{DNA}} = \frac{\beta^2 L}{D_2}\left\{\frac{K_0(\kappa a)}{\kappa a K_1(\kappa a)} + 4D_2\sum_{n=1}^{\infty}\Delta h_{2n}^{\text{DNA}}\right\} \tag{17}$$

Hence,

$$\left(\frac{\partial F_{\text{excess}}^{\text{DNA}}}{\partial \kappa}\right)_{T,V} = \frac{-\beta^2 L C^{\text{DNA}}(\kappa a)}{D_2\kappa} \tag{18a}$$

where

$$-C^{\text{DNA}}(\kappa a) = -1 + \frac{K_0^2(\kappa a)}{K_1^2(\kappa a)} + 4D_2\left(\frac{\partial(\sum_{n=1}^{\infty}\Delta h_{2n}^{\text{DNA}})}{\partial \ln \kappa}\right)_{T,V} \tag{18b}$$

In Figure 3 we plot $-C^{\text{DNA}}(\kappa a)$ as a function of κa. Whenever $\kappa a \geq 0.15$ or $C_S \geq 2 \times 10^{-3}$ M for DNA, appreciable corrections to the colligative properties of a line of charge model are necessary. If $\kappa a \geq 0.5$, we find a contribution to $C^{\text{DNA}}(\kappa a)$ due to deviations in the double helical charge distribution from cylindrical symmetry. Such effects are to be expected when the screening length is of the order of the pitch or smaller. Furthermore, corrections to cylindrical symmetry must also depend on the ratio of the pitch to the cylindrical radius. That is, for fixed κP whether or not the charge distribution appears uniform depends on how tightly wound the helical lines are. In the case of DNA double helix, P/a is 3.45 and $\kappa p = 1$ when $\kappa a = 0.3$. Thus, corrections to the uniform charge result arise in $C^{\text{DNA}}(\kappa a)$. On the other hand, an α helix has a pitch to radius ratio of 0.68, and $\kappa p = 1$ when $\kappa a = 1.5$. It is therefore not surprising that for $\kappa a < 2$ corrections to the uniform charge distribution are negligible in the α-helical case.

This section is concluded with a brief presentation of some corrected colligative properties for α-helical and DNA-type double helical charge distributions. We shall employ Manning's notation[2] and assume only monovalent mobile ions are present.

Define

$$\xi = q^2\{D_2k_BTb\}^{-1}$$

b is the linear spacing of the charges along the principal axis.

When $\xi < 1$, the activity coefficients γ_i of the mobile ions are[2]

$$\ln \gamma_i = \left(\frac{\partial F^\delta_{\text{excess}}}{\partial n_i}\right)_{T,V,n_{j\neq i}} \tag{19a}$$

Here "i" equal to 1 refers to counterion and 2 to coion; n_i is the number density of mobile ions of species "i", and $\delta = \alpha$, line, or DNA refers to the α helix, line of charge on the dielectric cylinder, and DNA double helical polyelectrolytes, respectively.

Now,

$$\left(\frac{\partial F^\delta_{\text{excess}}}{\partial n_i}\right)_{T,V,n_{j\neq i}} = \left(\frac{\partial F^\delta_{\text{excess}}}{\partial \kappa}\right)_{T,V}\left(\frac{\partial \kappa}{\partial n_i}\right)_{T,V,n_{j\neq i}} \tag{19b}$$

Consequently, we can write if $\xi < 1$

$$\ln \gamma_i = \frac{-\xi(X)(X+2)^{-1}}{2}C^\delta(\kappa a) \tag{19c}$$

Here $C^\alpha(\kappa a)$ is given by eq 12, $C^{\text{line}}(\kappa a)$ is given by eq 15, and $C^{\text{DNA}}(\kappa a)$ is obtained from eq 18b.

X is the ratio of the concentration of counterions from the polyelectrolyte, n_e, to the concentration of counterions from the simple salt, n_s. The mean activity coefficient $\gamma_\pm{}^\delta$ is:

$$\ln \gamma_\pm{}^\delta = \tfrac{1}{2}\{\ln \gamma_1 + \ln \gamma_2\} \tag{20a}$$

$$\ln \gamma_\pm = \frac{-\xi X(X+2)^{-1}C^\delta(\kappa a)}{2} \qquad \xi < 1 \tag{20b}$$

The osmotic coefficient ϕ^δ is related to the mean activity coefficient in the Deybe–Hückel approximation by[2]

$$\phi^\delta = 1 + \ln \gamma_\pm{}^\delta \quad \xi < 1 \tag{21a}$$

Employing eq 20b, we have

$$\phi^\delta = 1 - \frac{\xi X(X+2)^{-1}C^\delta(\kappa a)}{2} \tag{21b}$$

In the limit that $n_s \to 0$, $X \to \infty$ and $C^\delta(\kappa a) \to 1$. Denoting the salt-free osmotic coefficient by $\phi_p{}^\delta$, we have

$$\phi_p{}^\delta = 1 - \xi/2 \qquad \xi < 1 \tag{22}$$

in agreement with Manning.[2]

For $\xi > 1$, we proceed in an identical fashion as Manning does to find

$$\gamma_1{}^\delta = \frac{(\xi^{-1}X+1)}{(X+1)}\exp\left[\frac{-\xi^{-1}XC^\delta(\kappa' a)}{2(\xi^{-1}X+2)}\right] \qquad \xi > 1 \tag{23a}$$

$$\gamma_2{}^\delta = \exp\left[\frac{-\xi^{-1}XC^\delta(\kappa' a)}{2(\xi^{-1}X+2)}\right] \qquad \xi > 1 \tag{23b}$$

$$\kappa'^2 = \frac{4\pi q^2}{D_2k_BTb}(\xi^{-1}n_e + 2n_s) \tag{23c}$$

$$\phi^\delta = \left[\frac{-\xi^{-1}XC^\delta(\kappa' a)}{2} + \xi^{-1}X + 2\right][X+2]^{-1} \quad \xi > 1 \tag{24a}$$

$$\phi_p{}^\delta = (2\xi)^{-1} \qquad \xi > 1 \tag{24b}$$

A word of explanation with regards to eq 23a through eq 24b is appropriate. One of the referees has correctly observed that at high salt, $e\Psi/k_BT$ becomes small and for $\xi > 1$ the Poisson–Boltzmann equation can be linearized; i.e., condensation must actually disappear if the Poisson–Boltzmann description is correct. On the other hand, there is both theoretical[12] and experimental evidence[4] which indicates Manning theory predictions for the condensed charge fraction may be correct to at least 1.0 M. Thus, we regard eq 23a through eq 24b as a logical theoretical extension of Manning's original work; the equations demonstrate, within the context of a counterion condensation model, the influence of finite cylinder size and dielectric discontinuity on polyelectrolyte colligative properties.

By analogy to simple electrolyte theory, it seems appropriate to designate equations 19c through 24b as extended Manning colligative properties.

It follows from eq 21b, 22, and 24a,b that the so-called additivity rule[2]

$$\phi^\delta(n_e + 2n_s) = \phi_p{}^\delta n_e + 2n_s \tag{25}$$

holds only in the limit that $\kappa a \to 0$, i.e., $C^\delta(\kappa a) \to 1$. This conclusion casts further doubt on the interpretation of eq 25 which states that a fraction $(1 - \phi_p)$ of the counterions from the polyelectrolyte salt are bound to the polyion. Strictly speaking eq 25 is valid for helical polyelectrolytes when they appear as a line of charge, in other words at infinite dilution. However, as a matter of practical application, eq 25 is a useful approximation whenever $\kappa a \leq 0.15$.

Additional Observations

We conclude our discussion with several observations on Manning's counterion condensation theory. In his investigations, Manning replaces the actual flexible, linear polyelectrolyte by an infinitely thin line of charge. To the uninitiated and perhaps naive, ignoring the influence of the cylinder on the excess electrostatic free energy seems to be an approximation of questionable validity. Such a query provided part of the original motivation for this work. We therefore examined the colligative properties of helical polyelectrolytes and found when $\kappa a \geq 0.15$ a line of charge model is inadequate. On the other hand, when the screening length is large relative to a, the helical polyion appears as a line of charge and Manning's original treatment is appropriate. Consequently, we formulated a series of extended Manning colligative properties for all values of $\kappa a \leq 2$.

Acknowledgment. The author would like to thank Marshall Fixman for invaluable assistance and stimulating discussions throughout the course of this work. This work was supported in part by N.I.H. Grant GM 13556.

References and Notes

(1) J. Skolnick and M. Fixman, *Macromolecules*, **11**, 867 (1978).
(2) G. Manning, *J. Chem. Phys.*, **51**, 924, 3249 (1969).
(3) G. Manning and A. Holtzer, *J. Phys. Chem.*, **77**, 2206 (1973).
(4) G. Manning, *Biophys. Chem.*, **7**, 95 (1977).
(5) H. S. Kielman, J. M. A. M. van der Hoeven, and J. C. Leyte, *Biophys. Chem.*, **4**, 103 (1976), and references therein.
(6) J. M. Bailey, *Biopolymers*, **12**, 1705 (1973).

(7) D. Stigter, *J. Phys. Chem.*, **82**, 1602 (1978).
(8) A. D. MacGillivray and J. J. Winklemann, *J. Chem. Phys.*, **45**, 2184 (1966).
(9) A. D. MacGillivray, *J. Chem. Phys.*, **56**, 80, 83 (1972).
(10) A. D. MacGillivray, *J. Chem. Phys.*, **57**, 4071, 4075 (1972).
(11) J. Skolnick, Ph.D. Thesis, Yale University, 1978.
(12) J. M. Bailey, *Biopolymers*, **12**, 559 (1973).
(13) We are indebted to referee number two for pointing out the limitations of the infinite pitch helix model.
(14) D. Soumpasis, *J. Chem. Phys.*, **69**, 3190 (1978).
(15) We are grateful to a referee for supplying an additional reference to F. E. Karasz and T. L. Hill, *Arch. Biochem. Biophys.*, **97**, 505 (1962). Karasz and Hill derive the interaction between two point charges located inside a salt-excluding dielectric cylinder which has been placed in bulk salt solution. Ψ_T, given in eq 1a, is a limiting case of their treatment. As indicated previously,[1,11] when the point charges are brought from within to on the dielectric cylinder, the contribution of those terms which reflect the distortion of the lines of flux due to a dielectric discontinuity becomes important.

Structure and Viscosity of Poly(dimethylsiloxanes) with Random Branches

Enrique M. Valles and Christopher W. Macosko*

Department of Chemical Engineering and Materials Science, University of Minnesota, Minneapolis, Minnesota 55455. *Received May 17, 1978*

ABSTRACT: Viscosity rise and extent of reaction were followed during the stepwise polymerization of vinyl-terminated poly(dimethylsiloxane) with tri- and tetrafunctional hydrosilanes. Gel point results and M_w data by light scattering agree with predictions from branching theory. This indicates that the influence of side reactions, substitution effects, and ring formation is small. The bulk viscosity of the branched molecules was found to correlate with the weight average molecular weight of the longest linear chain through the molecules, $M_{L,w}$, and with gM_w, where g is the ratio of branched to linear polymer radii of gyration.

A major area of study of the physics of polymer science is the one concerned with the relations between measurable viscoelastic properties and molecular parameters. One of the best known relations in this area is the one that correlates the zero shear rate viscosity of polymer melts to their average molecular weight. If the polymer is linear,

$$\eta_0 = KM_w^a \quad (1)$$

with $a = 3.4$ for $M_w > M_c$ and $2.5 \geq a \geq 1.0$ for $M_w < M_c$, where K is a temperature-dependent constant, η_0 is the zero shear rate viscosity, M_w is the weight average molecular weight, and M_c is the critical molecular weight beyond which the influence of entanglements begins to be important. Equation 1 applies to all common polymers, both in bulk and in concentrated solution.[1]

For branched systems the relation between η_0 and the molecular parameters is not so well established. The introduction of a few long branches seems to decrease the viscosity of the polymer if it is compared with the linear polymer of the same molecular weight.[2-7] However, when the branches are long enough to form many entanglements, the viscosity of the branched system is higher than that of the linear polymer of the same molecular weight.[8-11]

Graessley[11] has recently reviewed the effect of long branches on η_0 for model branched materials, four- and six-arm star molecules. He finds a good correlation for the viscosity data with

$$\eta_0 = K(gM_w)^a \quad (2)$$

where $a \simeq 3.4$, the same as for the linear case, and g is the ratio of the squares of the radii of gyration of a branched to the linear chain of the same M_w, s_b^2/s_l^2. Thus $g \leq 1$ and decreases with increased branching. Graessley finds that eq 2 holds up to $gM_w \simeq 2 \times 10^5$. At higher gM_w values, presumably when the branches entangle, η_0 rises even more steeply for these branched polymers as has been observed in other systems.[8-10]

Randomly branched molecules, rather than regular stars, are the type which occur in most commercial polymerizations. However, their structure, and thus g, is difficult to determine. By step-reaction polymerization a randomly branched system of known structure can be obtained using a polyfunctional comonomer. In this work we have studied the viscosity rise during polymerization of a well-defined system composed of long molecules of bifunctional poly(dimethylsiloxane) with reactive groups at their ends and small trifunctional and tetrafunctional molecules. First we describe this polymerization system and our experimental methods. Then we use the branching theory to relate the viscosity rise data to the changing structure of the reacting system.

Table I
Reactants

c	formula	mol wt M_n	M_w/M_n (GPC)
B_2	$ViPhCH_3SiO(Si(CH_3)_2O)_n$-$SiCH_3PhVi$	11600[a]	2.21
B_2'	$ViPhCH_3SiO(Si(CH_3)_2O)_n$-$SiCH_3PhVi$	33400[b]	2.60
A_4	$(HSi(CH_3)_2O)_4Si$	329	
A_3	$(HSi(CH_3)_2O)_3SiPh$	330	
A_2	$H(CH_3)_2SiOSi(CH_3)_2H$	134	

[a] By vinyl titration (ref 14); average of six titrations ranging from 11 200 to 12 000. [b] Same as *a* with three titrations ranging from 31 500 to 34 800. [c] Reactant identification.

Experimental Section

The Chemical System. Polymerization between long molecules of end-vinyl-substituted poly(dimethylsiloxane) and silanes of three different functionalities were studied. A complete listing of the chemicals used, together with their average molecular weights and molecular weight distributions, is given in Table I. As an example, the reaction between the vinyl-terminated

0024-9297/79/2212-0521$01.00/0